Identification and quantification of ageing mechanisms in Li-ion batteries by Electrochemical impedance spectroscopy.

Erika Teliz[1,2], Fernando Zinola[2], Verónica Díaz[1]*

[1] Instituto de Ingeniería Química, Núcleo Interdisciplinario Ingeniería Electroquímica, Facultad de Ingeniería, Universidad de la República (UdelaR), J. Herrera y Reissig 565, CP 11300, Montevideo, Uruguay.
[2]Laboratorio de Electroquímica Fundamental, Núcleo Interdisciplinario Ingeniería Electroquímica, Facultad de Ciencias (UdelaR), Universidad de la República, Igua 4225, CP 11400, Montevideo, Uruguay.

Corresponding author: Dra. Verónica Díaz

Email:verodiaz@fing.edu.uy

Abstract

The transportation sector reported almost a quarter of global CO_2 emissions. Thus, efforts to decarbonize this sector are essential to achieving net zero emission goals. Among the actions to mitigate the effects of climate change in favor of decarbonization, lithium-ion electric vehicle market has expanded over the past years because of both scientific advances and encouraging public policies.

The analysis of ageing in lithium-ion batteries is essential to ensure optimal performance and determine the end of useful life for that purpose. The degradation of lithium-ion batteries is a complex multi-causal process. The ageing mechanisms could be grouped mainly into three degradation modes: Loss of Conductivity (CL), Loss of Active Material (LAM) and Loss of Lithium Inventory (LLI). Ageing battery or state of health was tracked based on capacity and power. Through the state of health (SoH) the degradation of the battery is quantified based on the decrease in capacity. However, the definition of SoH does not include an indication of the underlying deterioration mechanisms causing the degradation. Combined with electrochemical impedance spectroscopy (EIS), degradation modes can be identified and quantified non-destructively with the aim of find the correlation between their evolution with SoH.

This paper proposes a method to identify and quantify the ageing mechanisms in commercial 18650 NMC lithium-ion batteries over time using the EIS technique. The EIS spectra were fitted to the equivalent electrical circuit. Through the variation of the calculated parameters with time, the main mechanisms responsible for the degradation are identified, associating the Rohm increases with CL, Rsei and Rct with LLI and Rw with LAM respectively. Correlation between degradation modes with SOH were reported.

Keywords: lithium-ion battery; degradation mode; electrochemical impedance spectroscopy; ageing, SOH

1. Introduction

Mitigation of climate change is a key pressing problem we are facing today. Addressing this problem will require decarbonization of energy systems, particularly, those related to mobility. Achieving zero emissions in the transportation sector confronts us with new related challenges which involves investigation and development in energy electrochemical storage in batteries.

The use of Lithium-ion batteries in electrical vehicles is expanding very fast. However, it remains a considerable amount of research regarding degradation mechanisms and ageing modes with regards transport applications to predict remaining lifetime based on the development of battery models [1-7].

Ageing mechanisms are usually classified into three degradation modes named as: Loss of conductivity (CL), Loss of Lithium Ion (LLI) and Loss of Active Material (LAM) [8-9]. Loss of Lithium inventory denotes lithium ions consumption due to decomposition reactions, SEI layer growth and lithium plating. Loss of active material refers to the fact that active materials of anode and cathode are no longer available due to structural disarranging, particle cracking, graphite exfoliation, loss of electrical contact due to passivation surface layers. Characterization of ageing effects is very important meanwhile the quantification of the evolution of each degradation mode over the time has the potential to predict the remaining capacity and the amount of energy stored in the battery for each time. Several electrochemical techniques have been widely explored in investigations to identify and quantify degradation mechanisms [10-17]. Previous works [15-18] have demonstrated the potential of Electrochemical Impedance Spectroscopy (EIS) to identify ageing mechanisms in LIBs implementing this technique online as well as offline. Electrochemical Impedance Spectroscopy is a robust electrochemical technique which allows to recognize and track the evolutions of lithium-ion battery degradation processes. The advantage of EIS for characterization of ageing mechanisms is the large amount of information it can provide for understanding degradation modes.

Concerning NMC cathode chemistry, numerous outcomes were stated in literature. Several authors [19-23] addressed the increase of ohmic resistance to electrolyte decomposition and attributed to SEI layer growth the increase of impedance in the mid-frequency range of the spectra. Jalkanen et al. [24] also ascribed the increase of ohmic resistance to electrolyte decomposition as well as assigned impedance increase in the mid-frequency region to processes such as: lithium plating, mechanical cracking, loss of cathode active material contact and SEI layer growth. Temperature effect was also studied by Buchberger et al. in [25]. At room temperature impedance rise in the Mid-frequency region of the spectra has been assigned to electrolyte decomposition and dissolution of metals from NMC cathode. The usual procedure followed to evaluate impedance spectra of Li-ion cells is by electric equivalent circuits model track by a Complex Nonlinear Least Square fitting [26]. Sun et al. [27] refers to first and Second-Order Equivalent Circuit Models. To analyze the spectroscopy response, these authors divide the impedance spectrum into four zones according to frequency regions, identifying the characteristic elements of each of them according to what is detailed below.

Model resistances are associated with some electrochemical phenomena and can be used as indicators for evaluating the state of health (SoH)of the battery and its evolution with time operating under different conditions [28]. An ohmic resistance (Rohm) in serie with an inductor (L) characterize the region in the spectra at ultra-high frequencies. The high-frequency region is characterized by the SEI structure. It is denoted by a SEI layer resistance (Rsei) connected with a constant phase element (CPEsei) in parallel. On the other hand, in the medium-frequency region a charge transfer resistance (Rct) is depicted while the low-frequency region is characterized by a Warburg element Zw. Both are connected in series in the model and in parallel with a CPE (CPEdl), representing the effect of the double-layer capacity.

The detection and quantification of ageing and degradation modes in li ion batteries during real-daily operation is still a goal in battery commonplace applications. Ageing and degradation mechanisms often imply complex processes in operating conditions, being affected by conduction cycles, temperature effects, resting time between cycles, etc. So, it is real a difficult task quantifies ageing and degradation effects to predict how much loss of capacity will occur under a different regime. In this work, EIS is applied to study degradation mechanisms on 18650 commercial NMC cells. Fitted parameters were correlated with the SOH.

2. Experimental

Life cycle tests and EIS measurements at room temperature were carried out to study the change of resistance values and analyze the corresponding degradation modes of lithium-ion batteries. The test samples are commercial 18650 NMC lithium-ion. The batteries studied were subjected to 800 charge/discharge cycles with a current intensity of 1 A and 3 A, respectively. Measurements were performed on the Gamry Interface 5000E™ potentiostat/galvanostat. EIS measurements were made at open circuit potential at 50% SOC at room temperature, sweeping a frequency range between 10kHz and 10mHz, with an amplitude of 5mV and taking 10 points per decade.

A Second-Order Equivalent Circuit Model reported by Sun [24] was employed to fit experimental EIS values.

The equivalent circuit model employed is divided into four sections, which is fully corresponded to the frequency division in the impedance spectrum shown in Figure 1.
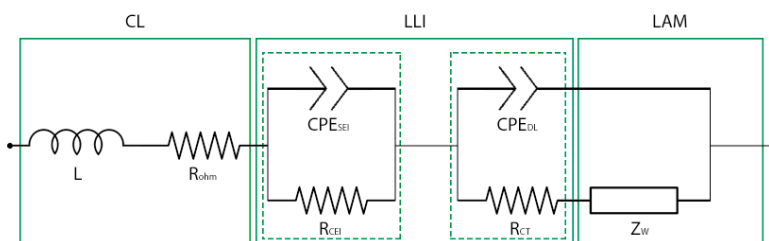
Figure 1. Equivalent Circuit Model

3. Results and Discussion

Figure 2 shows capacity evolution under experimental load profile with cycle numbers in the ageing processes.
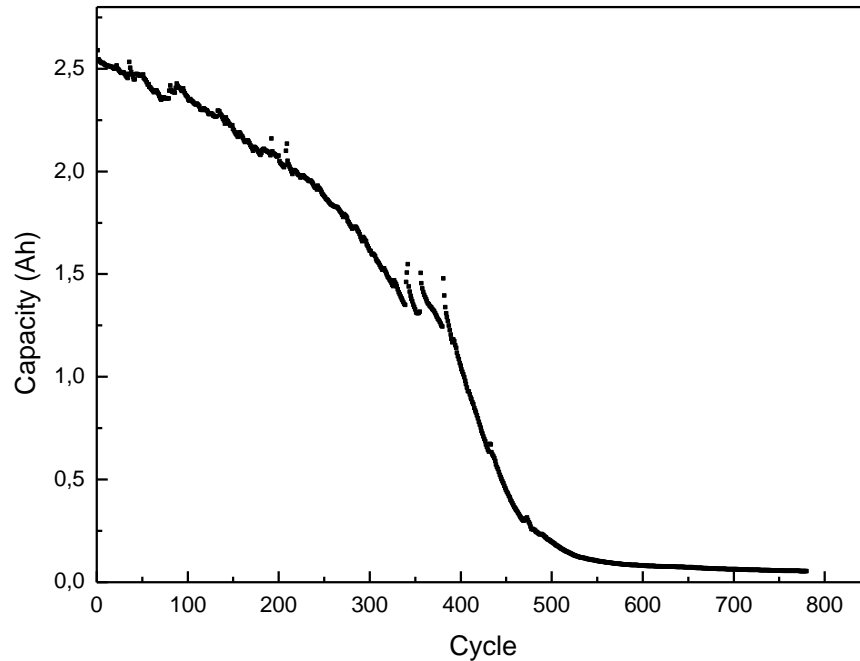
Figure 2. Capacity evolution.
During the test, the capacity of the tested cell is found to decrease due to degradation phenomenon. It is worthwhile noticing that different capacity fade rates were observed. The sample reaches 80% of SOH in the cycle 200, 60% in the cycle 300, 40% in the cycle 400 and 8% in cycle 500. In the first 200 cycles, capacity fade rate reported was: 0.25Ah/100 cycles. Between cycles 200 and 400, capacity fade rate increases achieving a value of 0.5 Ah/100 cycles. Finally in the last 100 cycles reported capacity fade still increase reaching 0.85Ah/100 cycles.

EIS measurements represented as Nyquist plots are depicted in Figure 3.
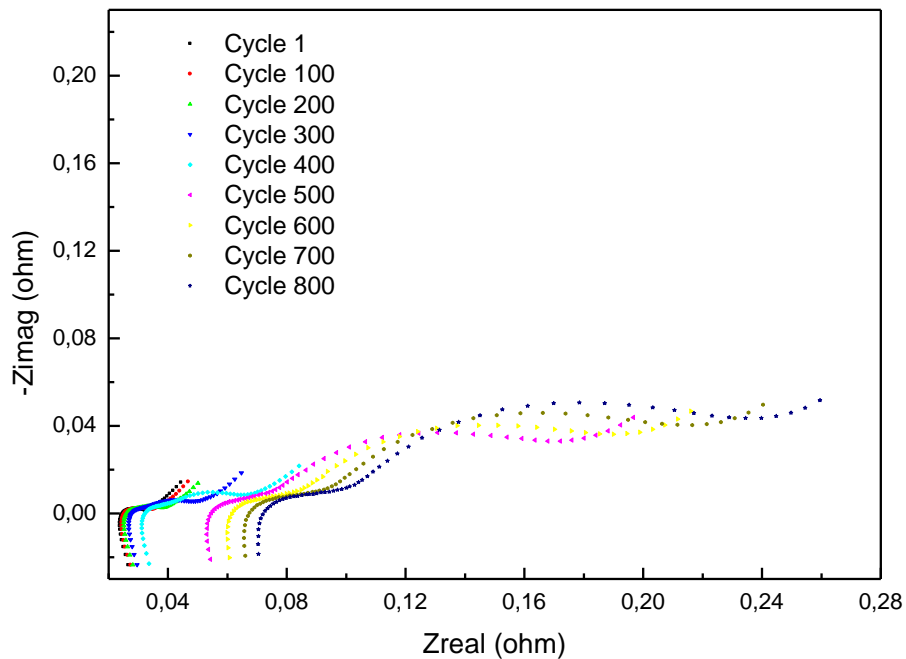
Figure 3. Nyquist plots, evolution with ageing during cycles

Impedance parameters were obtained by fitting from a second model equivalent model. Each Nyquist plot depicted four regions which correspond to the frequency division in the impedance spectrum (ultrahigh, high, medium, and low frequency). Plots shows an inductive structure in ultra-high frequencies where L is an inductor introduced by the current collector and Rohm explains the voltage drop due to the current collectors and the resistance due to the lack of contact between the binder, the electrode particles, and the electrolyte. All of them are related to the degradation mode denoted as conductivity loss (CL). Corrosion of connectors and current collectors, changes in the electrolyte cause CL due ageing. Besides Nyquist plots depict two depressed semi-circle at high and medium frequencies and an inclined line at low frequency attributed to Warburg impedance. Medium and high frequencies regions are represented by SEI and Charge Transfer structures respectively. The formation of SEI hinders the transfer of lithium ions between the electrodes. Moreover, the amount of intercalated and deintercalated lithium ions during the charge/discharge process is reduced. The irreversible loss of lithium ions decreases the lithium-ion concentration making charge transfer process more difficult. Thus, Rsei as well as Rct are related to LLI [28-29]. Warburg impedance, Zw stands for the diffusion impedance of lithium ions in the electrode solid particles. Warburg impedance models the lithium-ion diffusion process

in the bulk. Warburg impedance allows determination of the kinetics of this limiting process at low frequencies. Warburg impedance is defined as:

$$Z_w = \sigma\, w^{-1/2}\, (1 - j)$$

$$Y_0 = \frac{1}{\sigma\sqrt{2}}$$

Lithium ion diffusion coefficient D_{Li} can be calculated using the following equation [30]

$$D_{Li} = \frac{R^2 T^2 Y_0^2}{A^2 C^2 n^4 F^4}$$

where D_{Li} represents lithium diffusion coefficient, R is the gas constant, T is the absolute temperature, C is the lithium concentration in the cathode material, n is the number of electrons transferred per molecule, F is the Faraday's constant, A is the electrode surface area and Y_0 (S.s$^{1/2}$) is previously defined in the Warburg (infinite) impedance as a function of Warburg coefficient σ

Diffusion of the lithium ion within the electrolyte and active electrode materials would be controlled by the diffusion coefficient that relates to the particle size and available surface area of the electrode material. This point out that LAM is related to Diffusion coefficient, thus to Y_0.. During ageing processes, Y_0 decreases so it could be concluded diffusion coefficient also decrease because of LAM degradation mode.

To quantify the degradation and attribute the effect of each of the modes, the following parameters are defined [17]:

$$CL = 100\frac{(R_{ohm,n} - R_{ohm,1})}{R_{ohm,1}} \qquad \text{(eq. 1)}$$

$$LLI = 100\frac{(R_{SEI,n} + R_{Ct,n}) - (R_{SEI,1} + R_{Ct,1})}{R_{SEI,n} + R_{Ct,n}} \qquad \text{(eq. 2)}$$

For LAM we propose:

$$LAM = 100\frac{(Y_{0,1} - Y_{0,n})}{Y_{0,1}} \qquad \text{(eq.3)}$$

Where the subscript n represents the different cycles during the ageing processes and subscript 1 corresponds to the initial cycle, the battery freshly state

During the first cycles in ageing process only one semi-circle in the impedance curve is shown. Based on the overlapping of two semi-circles it can be concludes that time constants of the internal processes associated with LLI are similar.

During the ageing process, Rohm, Rct and Rsei show a strong increasing trend, with a clear turning point at cycle 400 (Figure 4). These changes are consistent with the corresponding

ageing mechanisms. Figure 5 depicts the evolution of Y_0 with cycles. During ageing Y_0 decreases, consequently lithium diffusion coefficient also decreases. After obtaining each resistance value in the ageing stage, the degradation modes can be quantified by the relative change of its associated resistances as it was stated in eq (1-3).

Combined with the mechanism analysis previously detailed, we use Rohm to represent CL, Rsei and Rct to represent LLI and Y_0 to characterize LAM. Certainly, the ageing mechanisms included in each degradation mode cannot be completely described by these resistances.
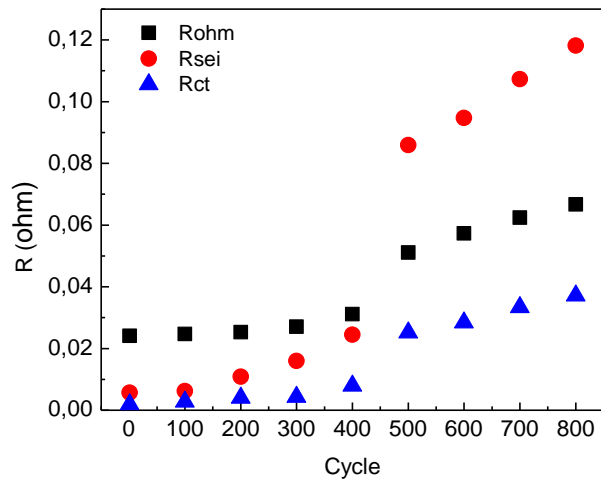
Figure 4. Evolution of EIS fitted resistances, Rohm, Rct, Rct with cycles
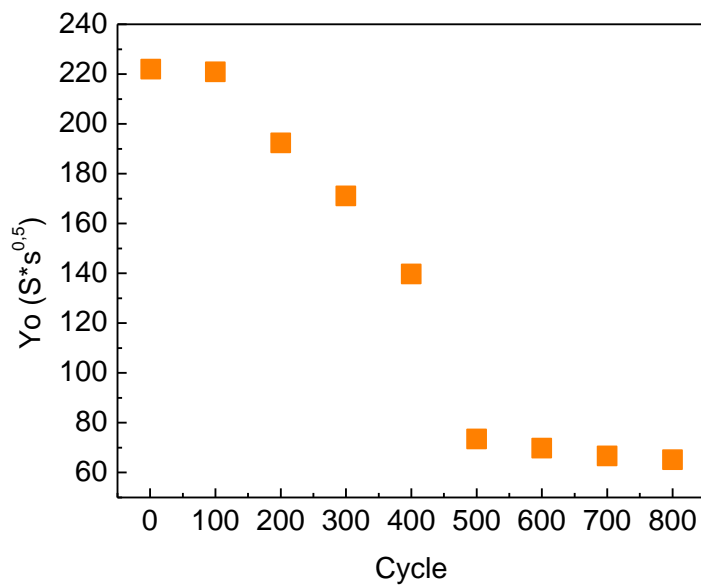
Figure 5. Evolution of Yo, resulted from EIS spectra fitting with cycles
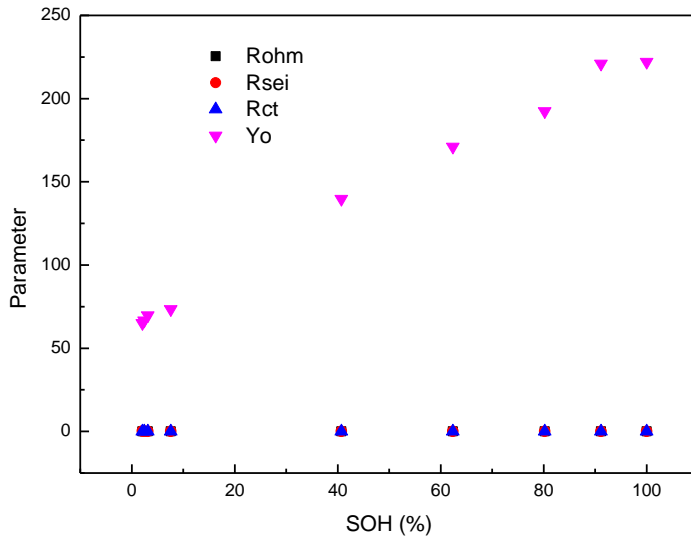
Figure 6. Evolution of EIS fitted parameters with cycles and SOH
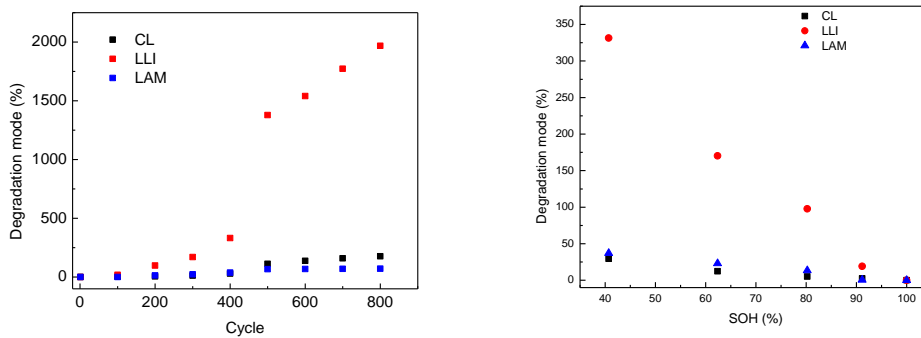
Figure 7. Evolution of degradation modes with cycles and SOH

Observing the quantitative results, we found that, as the ageing process progresses, resulted values of the three modes show a rising tendency. Compared with CL and LAM, LLI shows the most extensive increase. The fast growth of LLI is mainly attribute to the continuous growth of SEI films, which is also considered as the principal explanation for capacity fade.

It is worthwhile noticing that LAM and Y_0 evolutions show a linear correlation with the state of health of the battery in all the range. CL and LLI depict a linear behaviour for SOH values higher than 40%.

Figure 8 shows experimental and fitted values for linear correlation for degradation modes whereas Table 1 reports linear correlation results
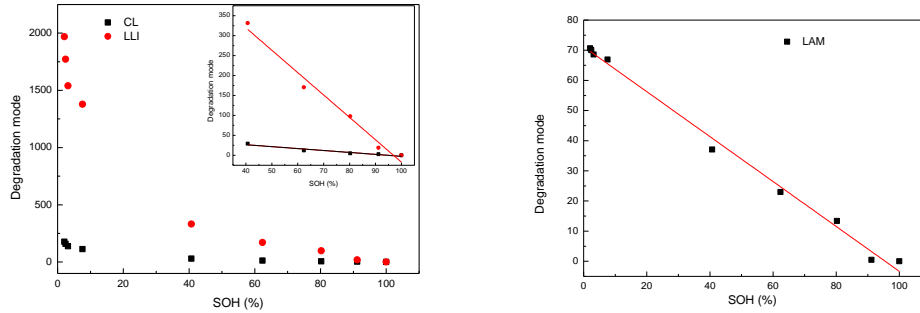
Figure 8. Linear correlation for DM and SOH.

Table1. Linear correlation results

Degradation Mode	Intercept	Slope	Pearson´s r	Adj R-Square
CL	46.09	-0.48	-0.99	0.98
LLI	544.3	-5.62	-0.97	0.92
LAM	71.16	-0.75	-0.99	0.99

4. Conclusions

This paper identifies and quantifies the ageing mechanisms in commercial 18650 NMC lithium-ion batteries over time using the EIS technique. The EIS spectra were fitted to the second order equivalent electrical circuit model. Through the variation of the calculated parameters with time, the main mechanisms responsible for the degradation are identified, associating the Rohm increases with CL, Rsei and Rct with LLI and Rw with LAM respectively.

The shapes of the impedance spectra show dissimilar transformation tendencies during the ageing process.

During the first cycles, there are not two distinguishable semi-circles in the medium-high frequency region. The overlap of two semi-circles indicates the time constants of the internal processes are similar.

The quantification methods presented not only ensure the corresponding relationship between degradation modes and resistance characteristics but also allow quantitative analysis under different conditions.

It was verified by experiments that, LLI always dominates the ageing process.

LAM depicts a linear correlation with SOH for all values, though CL and LLI show a linear behaviour for SOH values higher than 40%.

5. References

[1] M. Varini, P.E.Campana , G.Lindbergh, A semi-empirical, electrochemistry-based model for Li-ion battery performance prediction over lifetime, Journal of Energy Storage. 25 (2019), 100819, https://doi.org/10.1016/j.est.2019.100819.

[2] M.A. Hannan, M.H. Lipu, A. Hussain, A. Mohamed, A review of lithium-ion battery state of charge estimation and management system in electric vehicle applications: challenges and recommendations, Renew. Sustain. Energy Rev. 78 (2017) 834–854.

[3] V. Ramadesigan, P.W. Northrop, S. De, S. Santhanagopalan, R.D. Braatz,V.R. Subramanian, Modeling and simulation of lithium-ion batteries from a systems engineering perspective, J. Electrochem. Soc. 159 (3) (2012) R31–R45.

[4] J. Schmalstieg, S. Käbitz, M. Ecker, D.U. Sauer, A holistic ageing model for Li(NiMnCo)O2 based 18650 lithium-ion batteries, J. Power Sources 257 (2014) 325–334.

[5] S. Panchal, M. Mathew, R. Fraser, M. Fowler, Electrochemical thermal modelling, and experimental measurements of 18650 cylindrical lithium-ion battery during discharge cycle for an EV, Appl. Therm. Eng. 135 (2018) 123–132.

[6] M. Astaneh, R. Dufo-López, R. Roshandel, F. Golzar, J.L. Bernal-Agustín, A computationally efficient Li-ion electrochemical battery model for long-term analysis of stand-alone renewable energy systems, J. Energy Storage 17 (2018) 93–101.

[7] S.L.Hahn, M.Storch, R.Swaminathan, B. Obry, J.Bandlow, K.Peter Birke,Quantitative validation of calendar ageing models for lithium-ion batteries, Journal of Power Sources 400 (2018) 402-414., https://doi.org/10.1016/j.jpowsour.2018.08.019 .

[8] P. Iurilli, C. Brivio, V. Wood, On the use of electrochemical impedance spectroscopy to characterize and model the ageing phenomena of lithium-ion batteries: a critical review, Journal of Power Sources 505 (2021) 229860. https://doi.org/10.1016/j.jpowsour.2021.229860.

[9] J. Vetter et al., "Ageing mechanisms in lithium-ion batteries," J. Power Sources 147 (1-2) (2005) 269–281, doi: 10.1016/j.jpowsour.2005.01.006.

[10] Y.Li, M.Abdel-Monem, R.Gopalakrishnan, M. Berecibar, E. Nanini-Maury, N.Omar, P.V.D. Bossche, J.V. Mierlo, "A quick on-line state of health estimation method for li-ion battery with incremental capacity curves processed by Gaussian filter", J. Power Sources 373 (2018) 40-53.

[11] T. Goh, M. Park, M. Seo, J.G Kim, W.K. Sang, "Capacity estimation algorithm with a second-order differential voltage curve for li-ion batteries with NMC cathodes", Energy 135 (2017) 257-268.

[12] G. Zubi, R. Dufo-López, M. Carvalho, and G. Pasaoglu, "The lithium-ion battery: State of the art and future perspectives," Renew. Sustain. Energy Rev. 89 (2018) 292–308, doi: 10.1016/j.rser.2018.03.002.

[13] C. Weng, Y. Cui, J. Sun, and H. Peng, "On-board state of health monitoring of lithium-ion batteries using incremental capacity analysis with support vector regression," J. Power Sources 235 (2013) 36–44, doi: 10.1016/j.jpowsour.2013.02.012.

[14] M. Berecibar, M. Garmendia, I. Gandiaga, J. Crego, and I. Villarreal, "State of health estimation algorithm of LiFePO4 battery packs based on differential voltage curves for battery management system application," Energy 103 (2016) 784–796, doi: 10.1016/j.energy.2016.02.163.

[15] W. Choi, H. C. Shin, J. M. Kim, J. Y. Choi, and W. S. Yoon, "Modeling and applications of electrochemical impedance spectroscopy (Eis) for lithium-ion batteries," J. Electrochem. Sci. Technol., 11 (1) (2020) 1–13, doi: 10.33961/jecst.2019.00528.

[16] I. J. Gordon, S. Genies, G. Si Larbi, A. Boulineau, L. Daniel, and M. Alias, "Original implementation of Electrochemical Impedance Spectroscopy (EIS) in symmetric cells: Evaluation of post-mortem protocols applied to characterize electrode materials for Li-ion batteries," J. Power Sources 307 (2016) 788–795, doi: 10.1016/j.jpowsour.2016.01.036.

[17] C. Pastor-Fernández, K. Uddin, G. H. Chouchelamane, W. D. Widanage, and J. Marco, "A Comparison between Electrochemical Impedance Spectroscopy and Incremental Capacity-Differential Voltage as Li-ion Diagnostic Techniques to Identify and Quantify the Effects of Degradation Modes within Battery Management Systems," J. Power Sources 360 (2017) 301–318, doi: 10.1016/j.jpowsour.2017.03.042.

[18] W. Choi, H.-C. Shin, J.M. Kim, J.-Y. Choi, W.-S. Yoon, Modeling and applications of electrochemical impedance spectroscopy (EIS) for lithium-ion batteries, J. Electrochem. Sci. Technol. 11 (1) (2020) 1–13, https://doi.org/10.33961/ jecst.2019.00528

[19] S.F. Schuster, et al., Nonlinear ageing characteristics of lithium-ion cells under different operational conditions, J. Energy Storage 1 (2015) 44–53, https:// doi.org/10.1016/j.est.2015.05.003.

[20] U. Westerhoff, K. Kurbach, F. Lienesch, M. Kurrat, Analysis of lithium-ion battery models based on electrochemical impedance spectroscopy, Energy Technol. 4 (12) (2016) 1620–1630, https://doi.org/10.1002/ente.20160015.

[21] P. Aurora, N. Ramaswamy, T. Han, K. Adjemian, Electrochemical impedance spectroscopic analysis of lithium-ion battery ageing mechanisms, ECS Meet. Abstr. (2013), https://doi.org/10.1149/MA2013-01/4/254.

[22] Choi, W.; Shin, H.C.; Kim, J.M.; Choi, J.Y.; Yoon, W.S. Modeling and Applications of Electrochemical Impedance Spectroscopy (EIS) for Lithium-ion Batteries. J. Electrochem. Sci. Technol. 11 (2020) 1–13, doi:10.33961/jecst.2019.00528.

[23] R. Xiong, J. Tian, H. Mu, C. Wang, A systematic model-based degradation behavior recognition and health monitoring method for lithium-ion batteries, Appl. Energy 207 (2017) 372–383, https://doi.org/10.1016/j.apenergy.2017.05.124.

[24] K. Jalkanen, J. Karppinen, L. Skogstrom, ¨ T. Laurila, M. Nisula, K. Vuorilehto, Cycle ageing of commercial NMC/graphite pouch cells at different temperatures, Appl. Energy 154 (2015) 160–172, https://doi.org/10.1016/j. apenergy.2015.04.110.

[25] I. Buchberger, et al., Ageing analysis of graphite/LiNi1/3Mn1/3Co1/3O2 cells using XRD, PGAA, and AC impedance, J. Electrochem. Soc. 162 (14) (2015) A2737, https://doi.org/10.1149/2.0721514jes.

[26] Illig, 'Physically Based Impedance Modelling of Lithium-Ion Cells', p. 231.

[27] Sun, H.; Jiang, B.; You, H.; Yang, B.; Wang, X.; Wei, X.; Dai, H. Quantitative Analysis of Degradation Modes of Lithium-Ion Battery under Different Operating Conditions. Energies 14 (2021) 350, https:// doi.org/10.3390/en14020350.

[28] Wang, X.; Wei, X.; Dai, H. Estimation of state of health of lithium-ion batteries based on charge transfer resistance considering different temperature and state of charge. J. Energy Storage 21 (2019) 618–631, doi:10.1016/j.est.2018.11.020.

[29] Pastor-Fernandez, C.; Widanage, W.D.; Marco, J.; Gama-Valdez, M.A.; Chouchelamane, G.H. Identification and quantification of ageing mechanisms in Lithium-ion batteries using the EIS technique. In Proceedings of the 2016 IEEE Transportation Electrification Conference and Expo (ITEC), Dearborn, MI, USA, 27–29 June 2016; pp. 1–6, doi:10.1109/ITEC.2016.7520198.

[30] J.Huang, Diffusion impedance of electroactive materials, electrolytic solutions and porous electrodes: Warburg impedance and beyond, Diffusion impedance of electroactive materials, electrolytic solutions and porous electrodes: Warburg impedance and beyond Electrochimica Acta 281 (2018) 170-188, https://doi.org/10.1016/j.electacta.2018.05.136

Acknowledgments